



1. Introduction

By 2024, Mexico has proposed the goal of producing 35% of electric power from non-fossil energy sources. This objective started a series of government policies focused on promoting the exploration, exploitation, development, and use of renewable energies.

In accordance with the Geothermal Energy Law promulgated by the Secretary of Energy (SENER), until June 2018, 24 exploration concessions for geothermal resources have been granted along Mexican territory. The geothermal area of Celaya is one of the 24 concessions to perform geophysical exploration of the subsurface to obtain information of some physical properties, which can be integrated with geology and geochemistry to determine the conceptual geothermal model and define the existence of the reservoir, extension area, volume, depth, temperature, etc.

Celaya geothermal area is located in the state of Guanajuato, at the central portion of Mexico. The stratigraphy of this area comprises a volcano-sedimentary sequence representing the hydrogeological basement. This Mesozoic unit is covered by miscellaneous volcanic deposits from the Miocene. At the top, a sedimentary cover comprised of alluvial and lacustrine deposits filling all the depressions on Celaya Basin (Alvis et al., 2019).

Between August and November 2017, the company *Energías Alternas* (ENAL—CARSO) in collaboration with the Center for Geosciences (CGEO) of the National Autonomous University of Mexico (UNAM), carried out the acquisition of 62 BMT stations (AMT/MT). Distances between MT stations vary from 500 m, in the central portion, to 3 km towards the ends of the area of interest. Each day, EM fields were measured at 4 different sites with Phoenix MTU-5A and V8 data loggers, recording MT data approximately for 2 (AMT) and 8 (MT) hours.

2. Area of Interest

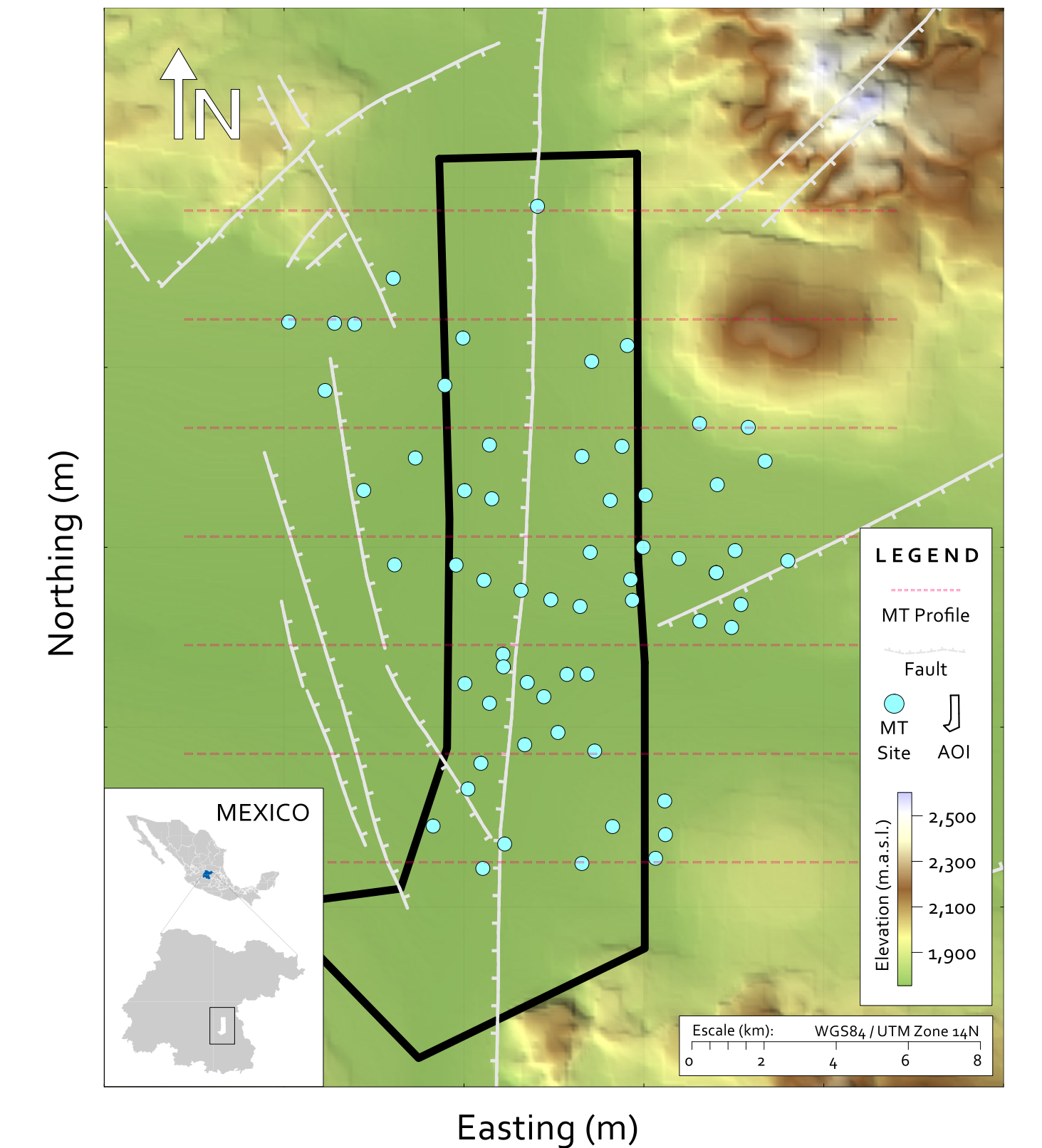


Figure 1. Location of MT sites

3. Data Processing

EM horizontal and vertical transfer functions were estimated applying a robust single-site (AMT) and a multivariate (MT) processing scheme, which allows to remove incoherent noise from data.

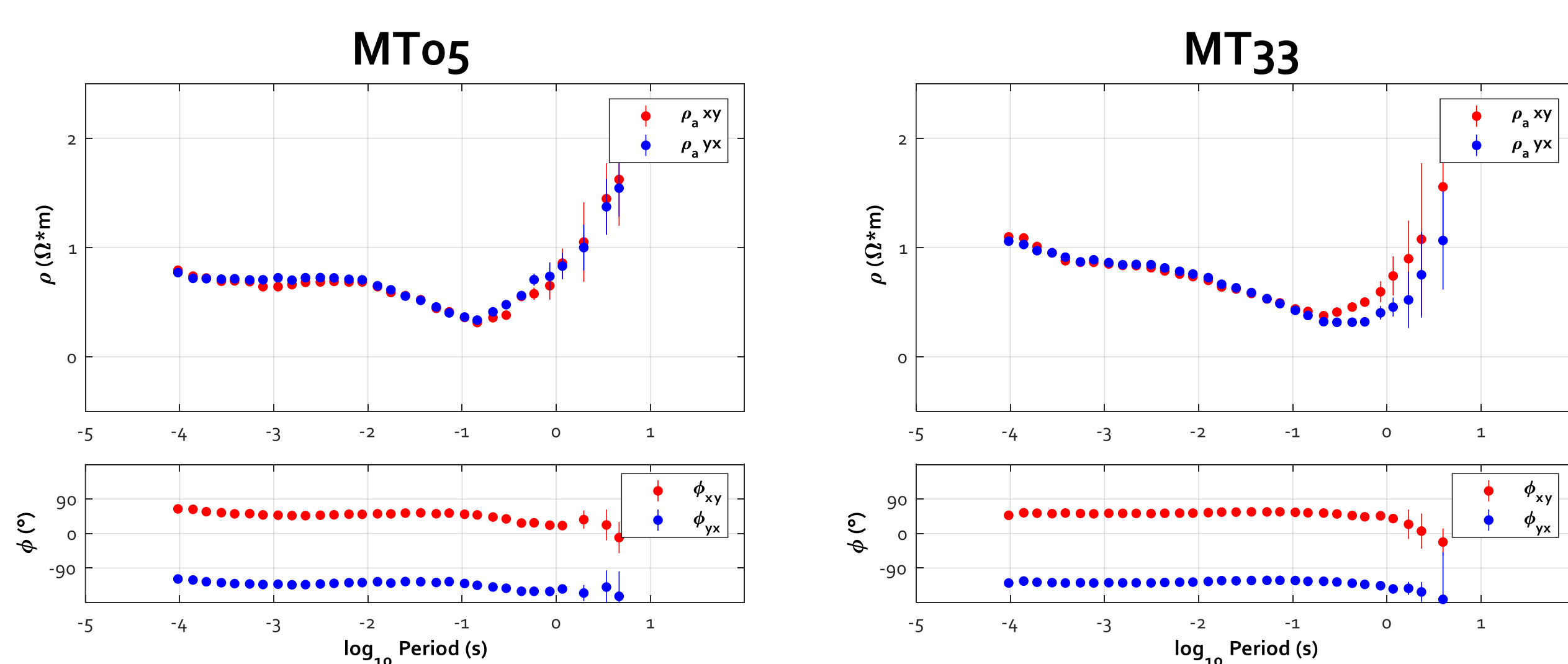


Figure 2. Apparent resistivity and phase curves for sites 05 and 33

Figure 2 shows the behavior from two different sites approaching a 1-D medium up to 10 Hz, whose resistivity values can be related to the sedimentary package. For longer periods, curves show a divergence and a notable increase in resistivity values which could be related to the igneous basement. This 1-D behavior is reaffirmed by the phase tensor ellipses (Caldwell et al., 2004), which shows circle shapes and skew angles (β) close to 0.

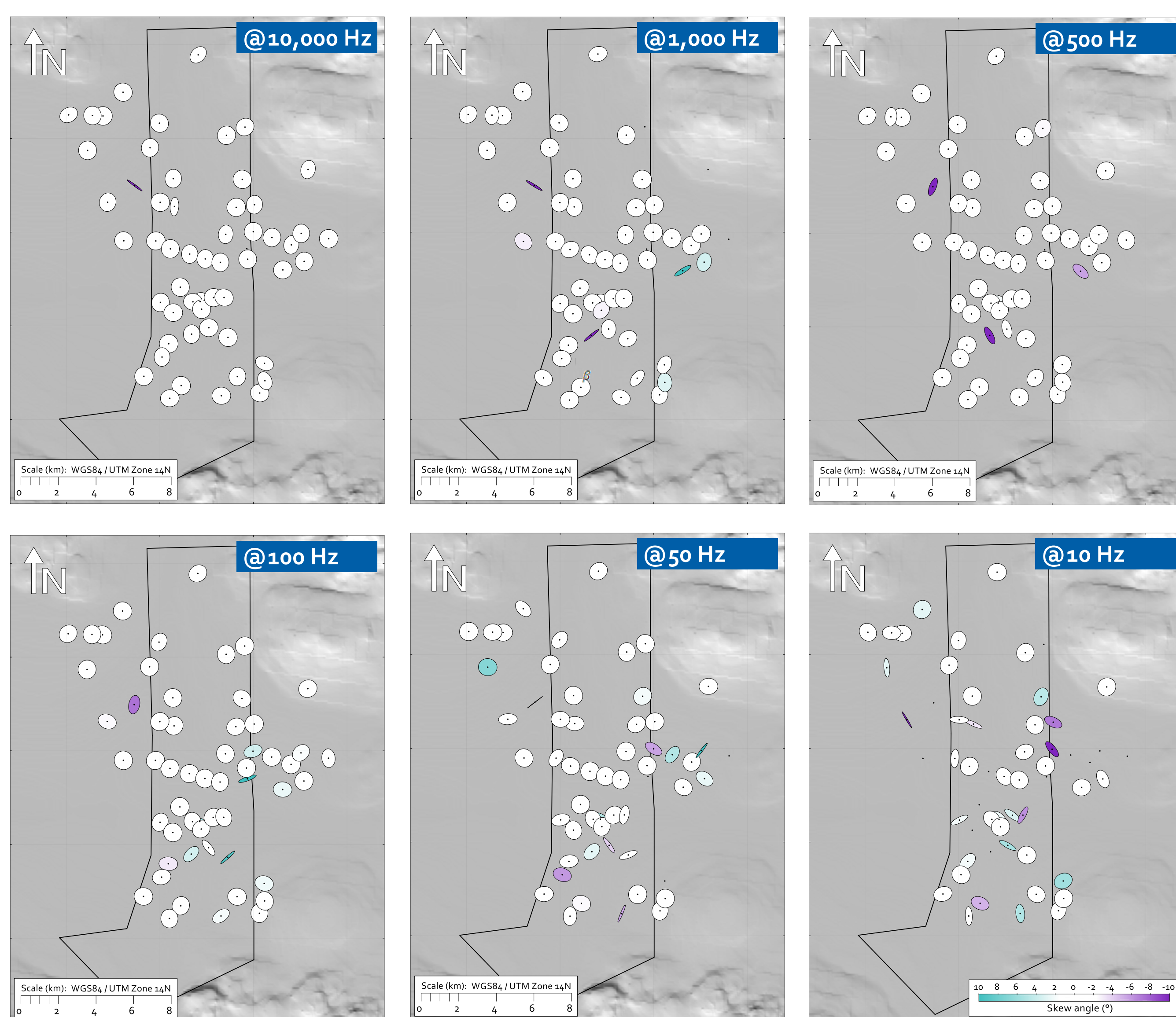


Figure 3. Phase tensor ellipses for MT sites

4. 3D Inversion results

3D inversions of MT data were carried out using ModEM (Kelbert et al, 2014). The grid configuration consists in a minimum cell size of 300m x 300m x 25m. Layer thickness increases with depth by a factor of 1.25. Starting resistivity model was an homogeneous halfspace of 100 Ω m. From the 62 MT sites, only 56 were used, omitting noisy soundings/periods with large scattering/large error bars. 2 schemes were proposed: a) data from the full impedance tensor and b) the Complex MT Apparent Resistivity Tensor (CART, Hering et al., 2019). 2D cross-sections from resistivity 3D-model from both schemes with a global RMS of ~2.2%, are presented.

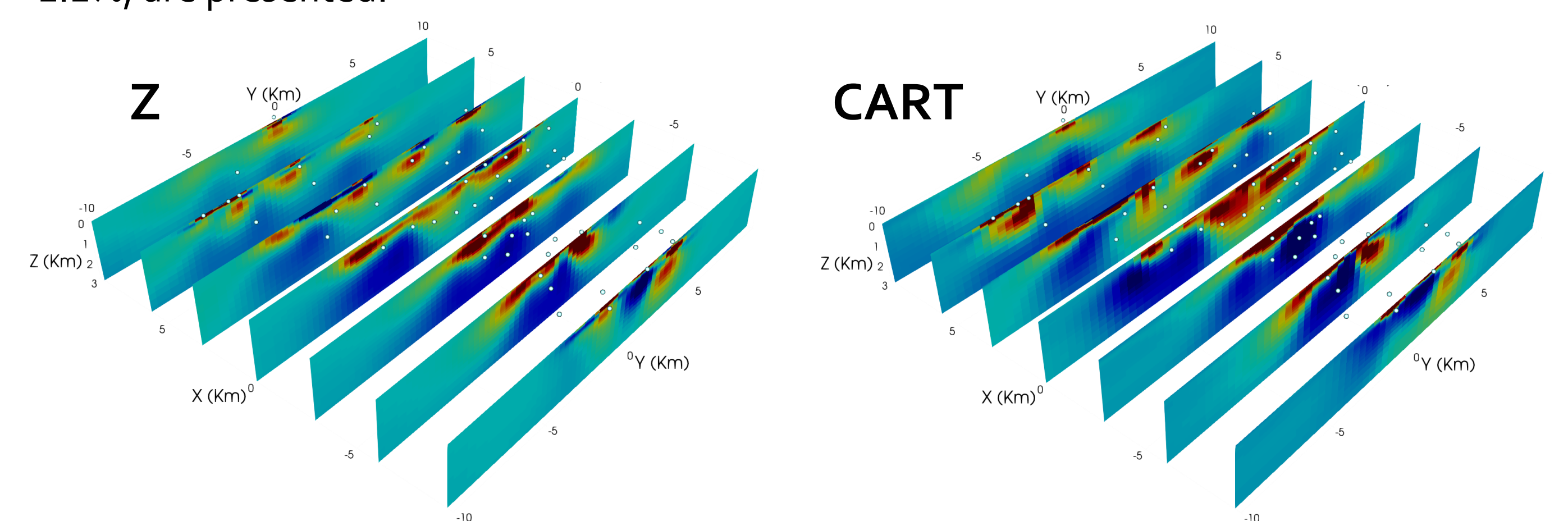


Figure 4. Resistivity models from the full impedance tensor (left) and CART (right) 3D inversions

Results from 3D inversion for both schemes show a conductive layer within the entire study domain overlying a more resistive unit. Principal differences between both inversion results can be observed in profiles $X = 0$ Km and $X = 3$ Km, while the other profiles show similarities between conductive and resistive structures. Besides, resistivity values results from CART seem a bit more pronounced. A 2D cross-sections from both schemes were compared with borehole stratigraphy, in which CART results show a better match delimiting the lower boundary for the conductive-sedimentary unit from CART inversion.

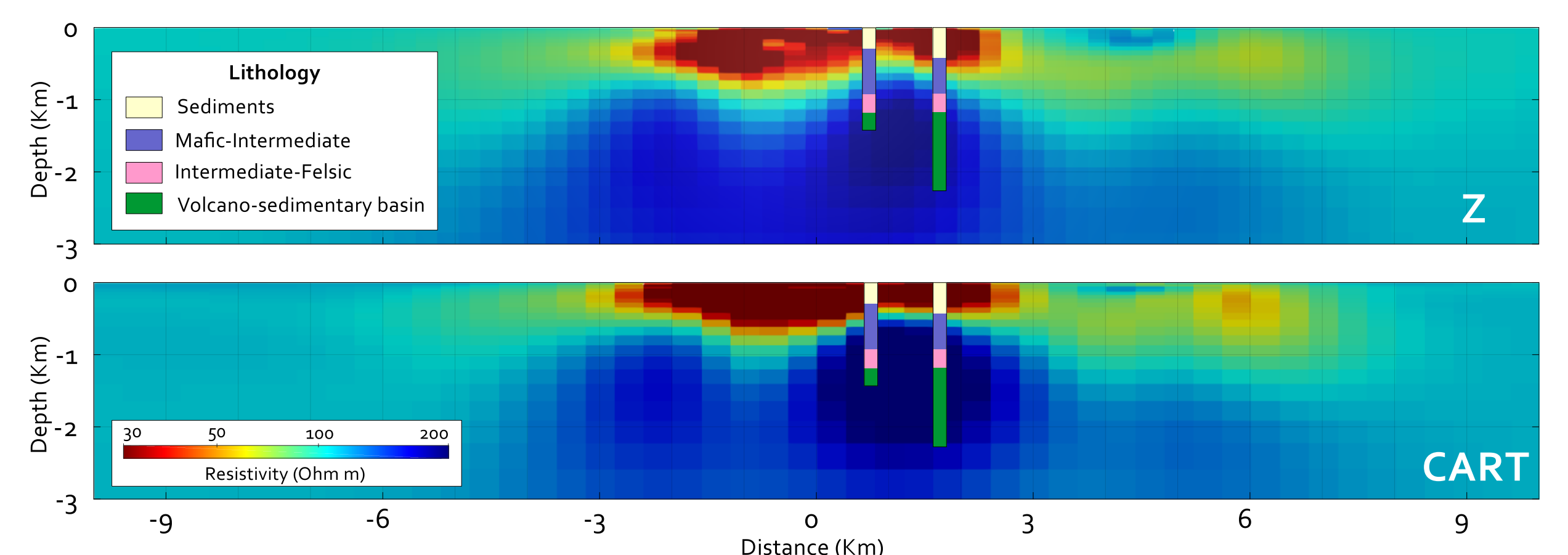


Figure 5. Correlation between resistivity and stratigraphy for Z and CART inversions

5. Conclusions and outlook

3D inversion results showed a first landscape about the conductivity distribution of underlying materials at Celaya geothermal area. As being the second attempt applying the 3D inversion of the CART in real data, several tests and inversion parameters combinations should be done to improve results for this model. However, CART profile showed in Figure 5 shows a better correlation between conductivity and lithology. Next steps include an improvement on the estimation of horizontal transfer functions and the use of tipper information in Z inversion to get and a new comparison between both schemes.

References

- Alvis, J., Carrera-Hernández, J., Levresse, G., and Nieto-Samaniego, A. (2019). *Assessment of groundwater depletion caused by excessive extraction through groundwater flow modelling: The Celaya aquifer in central Mexico*. Environmental Earth Sciences, 79(482), 1–22.
- Caldwell, G., Bibby, H., and Brown, C. (2004). *The magnetotelluric phase tensor*. Geophysical Journal International, 158(2), 457–469.
- Hering, P., Brown, C., and Junge, A. (2019). *Magnetotelluric Apparent Resistivity Tensors for Improved Interpretations and 3-D Inversions*. Journal of Geophysical Research—Solid Earth, 124, 1–28.
- Kelbert, A., Meqbel, N., Egbert, G., and Tandon, K. (2014). *ModEM: A modular system, for inversion of electromagnetic geophysical data*. Computers and Geosciences, 66, 40–53.

Acknowledgements

We would like to thank the Department of Exploration from *Energías Alternas* (ENAL – CARSO) for providing the data for this project. Also many thanks to the Geophysical Exploration group from Center for Geosciences of National Autonomous University of México (UNAM), especially to Dr. Fernando Corbo-Camargo for his support linking industry and academia.